

Infrared-Induced Reaction on MoO_3 Using a Tunable Infrared Free Electron Laser

Md Golam Moula,[1,2] Shinsuke Sato,[1,3] Katsumi Irokawa,[4] Hironobu Niimi,[1] Shushi Suzuki,[1] Kiyotaka Asakura,*[1] and Haruo Kuroda[4]

[1]Catalysis Research Center, Hokkaido University, 21-10 Kita, Kita-ku, Sapporo 001-0021

[2]Open School, Bangladesh Open University, Gazipur-1705, Bangladesh

[3]Quantum Science and Engineering, Graduate School of Engineering, Hokkaido University, 13-8 Kita, Kita-ku, Sapporo 060-8628

[4]IR-FEL Research Center, Institute for Science and Technology, Tokyo University of Science, 26412 Yamazaki, Noda 278-8510

Received November 6, 2007; E-mail: askr@cat.hokudai.ac.jp

We observed the IR-induced reaction of C_2H_5OH on MoO_3 using a pulsed and tunable infrared free electron laser (IR-FEL). The IR-FEL-induced reaction showed wavelength dependency and requires light stronger than a certain threshold level. The C_2H_5OH was converted mainly to C_2H_4 only when the MoO_3 was irradiated with focused IR-FEL at 967 and 814 cm^{-1} corresponding to Mo=O stretching modes, whereas IR light at 1200 cm^{-1} induced no reaction. The origin of this IR-FEL-induced reaction is discussed.

Metal oxide catalysts are promising for controlling chemical processes with high selectivity, e.g., selective oxidation of alkanes and small oxygenated molecules such as alcohols by gas-phase oxygen molecules. Unlike metal catalysts, metal oxide catalysts consist of two components: metal cations and lattice oxygen atoms. The former plays the role of a Lewis acid and the lattice oxygen plays a more important role in selective oxidation reactions in these oxide catalysts.[1] The lattice oxygen atoms can abstract the hydrogen from C–H bonds, sometimes with subsequent nucleophilic addition of lattice oxygen to produce oxygenated compounds. The gas-phase oxygen is used to reoxidize the metal oxides; it engenders a total combustion reaction if it is directly activated.[2] The catalytic properties of lattice oxygen depend on the properties of metal–oxygen bonds, which range from covalent to ionic bonds and have an anisotropic or asymmetric structure.

We clarify this point using an example: Mo is a typical component of selective oxidation catalysts like BiMoOx, CoMoOx, and Mo–V–Nb–Te–Ox. The simplest form of the molybdenum oxide catalysts, MoO_3, catalyzes propene to acrolein,[3,4] alcohol to aldehyde,[5] and methane to formaldehyde.[6] MoO_3 has a crystal structure as shown in Figure 1, and has five different Mo–O bond lengths.[7,8] In these reactions, MoO_3 exhibits catalytic anisotropy,[3] where the selectivity depends on the exposed crystal plane. Ziółkowski explained the catalytic anisotropy in terms of the Mo–O bond-strength model of active sites (BSMAS).[9,10] If one could excite a specific metal–oxygen bond of the catalyst surface, one could achieve high selectivity. The metal–oxygen bond is related to a specific vibrational mode in the infrared region. Therefore, infrared light tuned to each vibration mode can selectively stimulate each bond. Consequently, a reaction accompanied with that specific bond can be brought about selectively. This selectivity control is the root idea of this study. Stretching frequencies accompanying metal–oxygen bonds are located at 1000–400 cm^{-1}. For example, MoO_3 has 968 (B_u: MoO_1O_2, asymmetric), 814 (B_u: MoO_1O_2, symmetric), 560 (A_u: Mo–O_3, stretch), and 450 (B_u: Mo–O_3, stretch and bend) cm^{-1} vibration modes.[11,12] However, the vibration energy is readily dissipated to lattice phonon modes and heats the sample. It would be difficult to distinguish the infrared-induced photoreaction from the thermal one if we did not apply a special strategy.

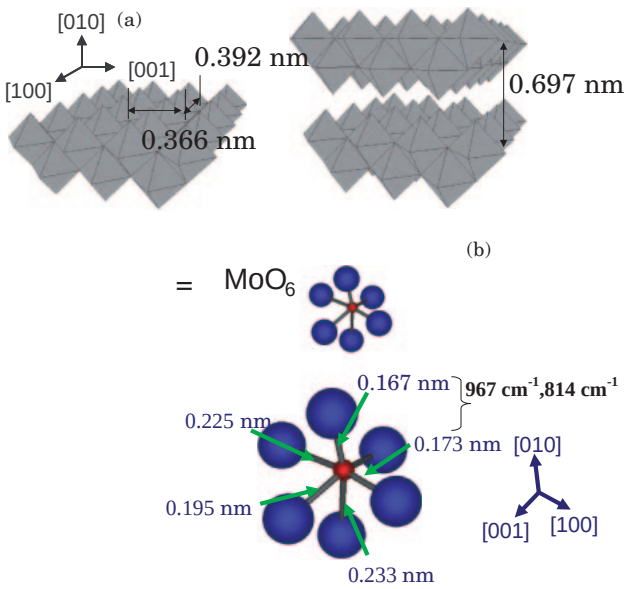

Figure 1. (a) Crystal and (b) molecular structures of MoO_3.

The simplest strategy to overcome this difficulty is to use a

Published on the web July 10, 2008; doi:10.1246/bcsj.81.836

short but intense IR-pulse irradiation with a long interval to prevent undesirable heating of the whole sample. A free electron laser (FEL) is the most suitable source for this purpose because it is wavelength-tunable and intense, having a pulse shape. The FEL is light emitted from the interference between light and relativistic electrons passing through a periodic magnetic field.[13,14] Recently, an IR-FEL facility dedicated to materials science was constructed at Tokyo University of Science (FEL-TUS).[15] The FEL-TUS possesses a high-powered (10 mJ) tunable IR laser (2000–600 cm^{-1}) with a short pulse width (2 μs per macropulse). We applied the free electron laser to assess the possibility of the selective excitation of Mo–O bonds in MoO_3 and to induce photoreaction of C_2H_5OH. In an earlier communication,[16] we reported that the IR-FEL can initiate a reaction by exciting the Mo–O bond selectively, where we claimed that this was the first case of inducing an infrared photoreaction on a solid catalyst surface through excitation of a specific vibrational mode. It is generally believed to be difficult because internal vibrational redistribution (IVR) of the vibrational energy is faster than the up-pumping rate, which is also limited by anharmonicities (anharmonic bottleneck). Recently, Liu et al. reported the resonant desorption of hydrogen from a Si surface by the resonant excitation of Si–H using an IR pulse generated from a free electron laser.[17]

We carried out further experiments to clarify the IR-induced chemical reaction on solid surfaces. Results of this study indicated that the IR-induced mechanism can not be explained by the simple picture described above, that the resonance frequency of IR simply excites the characteristic bond and provokes the reaction. We propose, based on our new experimental observations, that multiphoton absorption of IR photons, followed by the Mo–O bond break and the reduction of Mo^{6+}, is a key process for the present reaction.

Experimental

Materials. 99.5% MoO_3 was purchased from Kanto Chemical Co., Inc. and used without further purification. XRD indicated the crystallographic structure of *o*-MoO_3. The surface area was 1.3 $m^2\,g^{-1}$, as determined by a N_2 BET adsorption plot. Ethanol (99.5%; Wako Pure Chemical Industries Ltd.) was purified by freeze–pump–thaw cycles at 77 K over molecular sieves 3A.

Facility and Experimental Setup. FEL was emitted from an undulator of FEL-TUS at Noda campus of Tokyo University of Science. The details of the device have been described elsewhere.[15,18,19] The undulator is a vertical Harbach type of 43 periods with 32 mm period length. The maximum operating beam energy of the FEL-TUS is 40 MeV. An acceleration energy of 30.8 MeV was employed to merit stable IR generation at longer wavelengths. The FEL has two types of pulse structure. One is called macropulse (duration time 2 μs; the repetition is 2 Hz in this work) which is composed of a pulse train of micropulses (duration = 2 ps with a 350-ps period), as shown in Figure 2.

The IR-power depends on the wavelength and was measured using a power monitor (Gentec Co.). The details of the wavelength and the power used are summarized in Table 1. Three wavelengths were chosen for this measurement. The off-resonance frequency was 1200 cm^{-1}. The other frequencies were 967 and 814 cm^{-1}, which corresponded to the Mo=O symmetric and asymmetric vibrational modes, respectively as shown in Figure 1.[11,12,20] It is noteworthy that those wavelengths correspond to the valley of the gas-phase C_2H_5OH absorption band. The experimental setup is roughly sketched as shown in Figure 3. The original beam size was regulated by the IR exit window aperture size (45 mm). The FEL light was focused using a focusing mirror with 10 m focal length. The spot size was about 1 mm. The laser was further focused by a lens above the sample cell to about 0.1 mm^{ϕ}. By changing the vertical position of the sample, the laser-beam focus was finely adjusted on the sample.

We constructed a stainless steel sample cell to pretreat the sample and to perform infrared irradiation experiments. The cell was evacuated through a vacuum line using a turbo molecular pump (100 L s^{-1}). An IR window made of ZnSe was attached to an ICF flange that was cooled by water flow. The sample was loaded in a small stainless steel pan and mounted on a sample holder in the cell. It was heated to 800 K using a cartridge heater under the sample holder. The temperature was monitored using a thermo-

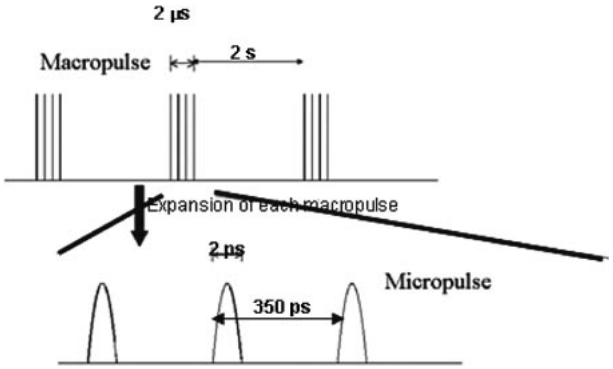

Figure 2. Pulse structure of FEL. 2 μs macropulse contains 2 ps micropulses.

Table 1. FEL-Power at Different Experimental Wavelength

Wavenumber /cm^{-1}	FEL-power[a)] /mJ $pulse^{-1}$	C_2H_4/mol	CH_3CHO/mol
1200	3.5	ND	ND
967	3.2	2.5×10^{-7}	1.1×10^{-7}
814	1.9	2.3×10^{-8}	ND
Thermal	—	ND	7.2×10^{-7}

a) The power was measured immediately above the lens set on an IR window made of ZnSe.

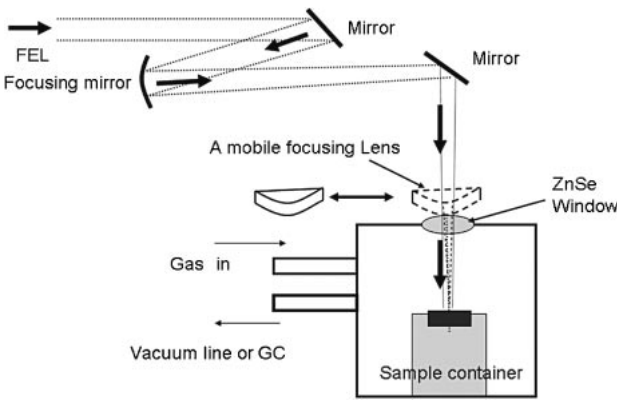

Figure 3. A schematic drawing of an experimental setup.

couple attached to the pan. Then, the sample cell was put on a three-axis stage with *x*, *y*, and *z* motions controlled using a personal computer. The positions were determined with 100-μm precision.

The MoO_3 was first calcined at 673 K for 2 h in the presence of oxygen and evacuated for 1 h at 673 K. After cooling the sample to room temperature in vacuo for more than 8 h, 6 Torr ethanol was introduced into the chamber and infrared irradiation was started. The pulse interval was 2 s to avoid heating the sample. No overall temperature increase was observed using the thermocouple. The sample was shifted horizontally after each five pulses to reduce effects of radiation damage. The gas phase was analyzed using gas chromatography (GC5A; Shimadzu Corp.) for C_2H_5OH, CH_3CHO, and C_2H_4 using a Porapak Q column and for CO, CO_2, and C_2H_4 using an active carbon column. The retention time and peak intensity were calibrated using corresponding standard gases.

The thermal reaction was carried out in the same cell in a batch reaction at a reaction temperature range of 403–443 K. The gas phase was analyzed using gas chromatography after 30 min reaction.

Characterization of the Irradiated Sample. The X-ray photoelectron spectroscopy (XPS) were measured using JPS 9200 (JEOL) in a micro-mode (field of view = 30 μm) with an Al Kα target at 20 kV–10 mA. The samples were taken from the IR reaction chamber and were loaded into the XPS chamber. During that procedure, the samples were exposed to air and measurements were carried out without further treatment. The binding energies were calibrated against bulk O1s photoelectron to be 530 eV.

Results

Reactions. Figure 4 shows gas chromatograms of C_2H_5OH reaction products on the MoO_3 sample after irradiation of 1200, 967, and 814 cm^{-1}. The samples were placed almost at the focusing condition using a focusing lens. When the sample was irradiated with 967 cm^{-1}, which is a resonant wavenumber to asymmetric stretching of $Mo(=O)_2$ bonds, the gas chromatography yielded peaks at 55, 68, 126, and 178 s which corresponded respectively to C_2H_4, H_2O, CH_3CHO, and unreacted C_2H_5OH. The gas chromatograms using an active carbon column in Figure 4b revealed C_2H_4 and CO_2 formation, the latter formation being 1/10 of the C_2H_4 formation. When the IR wavenumber was changed to 1200 cm^{-1}, which had no resonant vibration mode of MoO_3, we observed two peaks in the Porapak column corresponding to H_2O and C_2H_5OH; no peak was observed in the active carbon column. The reaction scarcely occurred at this wavelength. At 814 cm^{-1}, which is another resonance frequency of the symmetric stretching of $M(=O)_2$ bonds, we were able to observe production of C_2H_4. At that wavelength, the power was not so large, about 60% of that at 967 cm^{-1} and 50% of that at 1200 cm^{-1}. Although the production was small, we observed a distinctive amount of C_2H_4 and little formation of CO_2.

The thermal reaction was carried out at 403–443 K using the same sample cell in a batch reaction. The gas was sampled after 30 min of reaction. Figure 5 shows the gas chromatography output of the reaction at 413 K. The main product was CH_3CHO, as reported in the literature.[5] The activation energies are 24 kJ mol^{-1} as evaluated from Figure 5b. Even at 443 K no peak other than CH_3CHO was detected.

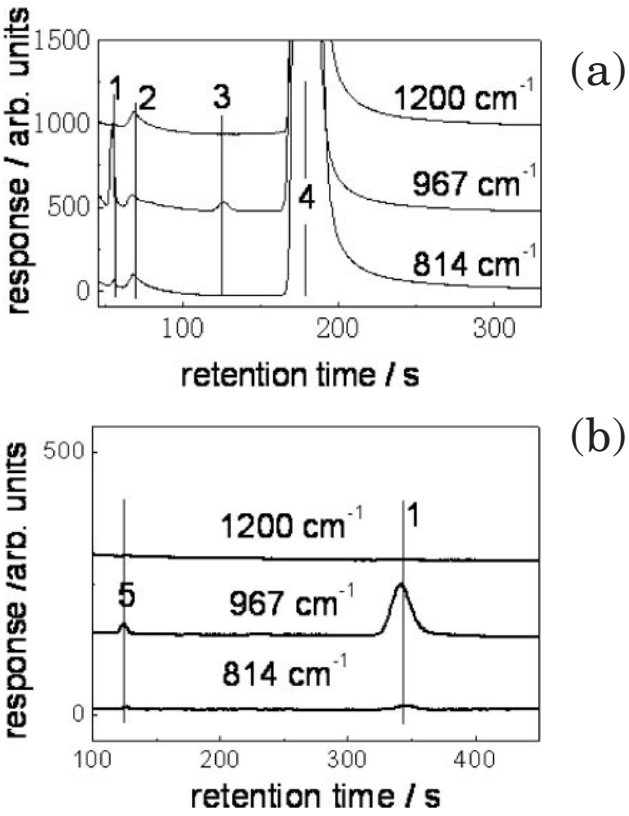

Figure 4. Gas chromatography analyses with different excitation wavelengths, using Porapak Q (a) and active carbon (b). 1, C_2H_4; 2, H_2O; 3, CH_3CHO; 4, C_2H_5OH; and 5, CO_2.

Table 1 lists the reaction products after IR-FEL irradiation and thermal reactions. The products were CH_3CHO and C_2H_4: C_2H_4 was the main product in the IR-induced reactions, whereas the CH_3CHO was formed in the thermal reaction. The amount of photons at the 967 cm^{-1} irradiation of Figure 4 was evaluated as 2×10^{17} photons per pulse from the power (3.2 mJ $pulse^{-1}$). We introduced 1800 macropulses into the sample. Consequently, about 4×10^{20} photons (0.7×10^{-3} mol) were introduced into the sample. The total converted C_2H_5OH was 3.6×10^{-7} mol. The apparent quantum yield was ca. 5×10^{-4} at 967 cm^{-1}.

To determine the product dependence on the intensity roughly, we changed the IR intensity by modifying the focus position. Figure 6 shows photographs of MoO_3 after irradiation and gas chromatography outputs using a Porapak column. We irradiated two infrared wavenumbers that were at 1200 and 967 cm^{-1} under different focusing conditions.

We decreased the power density of IR by removing the lens and increasing the focus size. Figures 6a and 6b respectively display photographs of MoO_3 after gently focused irradiation of FEL at 1200 and 967 cm^{-1}, using only a focusing mirror. The beam size was about 1 mm in diameter. We observed no product formation.

Figure 6c shows MoO_3 after irradiation with 1200 cm^{-1} FEL using a focusing lens, where beam size was about 0.1 mm^{ϕ} on the sample. We found a plume after every laser pulse shot, indicating the occurrence of optical breakdown. We also found holes in the sample after irradiation, as por-

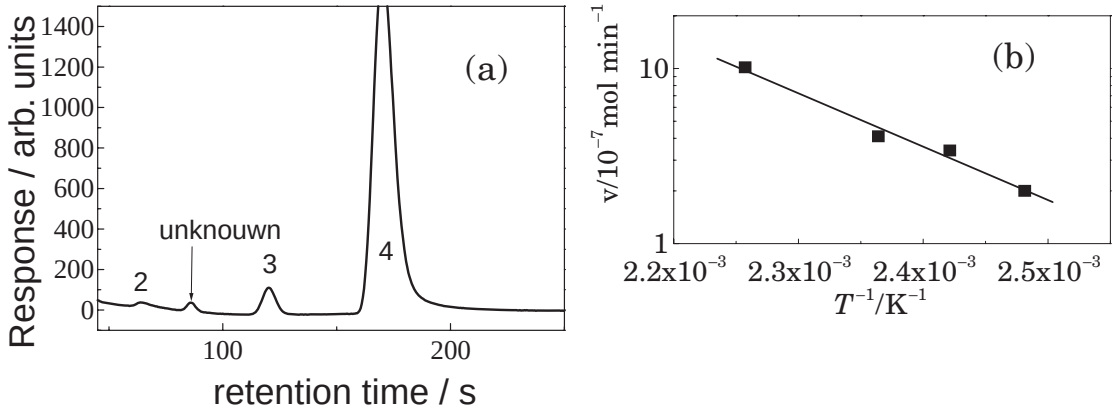

Figure 5. Gas chromatography output (a) for a thermal reaction at 453 K with a Porapak Q column: 2, H_2O; 3, CH_3CHO; and 4, C_2H_5OH and Arrhenius plot of CH_3CHO reaction rate against temperature.

trayed in Figure 6c. Because we moved the sample in a raster scan sequence to draw a rectangular shape, the corresponding rectangular holes were formed. The origin of the plume was plasma created by the high electric field of the FEL. However, gas chromatography gave only two peaks at retention times of 68 and 178 s, which corresponded to residual H_2O and unreacted C_2H_5OH, indicating that no reaction occurred, even in the presence of the FEL-induced plasma. We irradiated the sample twice in different positions A and B, almost at the focus position. We adjusted the vertical position of the sample to achieve a better focal point so that the photon density at the position of B was slightly higher than the position of A. We observed only trace amounts of CH_3CHO when irradiated at position B, as shown in Figure 6c-B though it is difficult to evaluate the formation amount quantitatively.

Figure 6d shows photographs of MoO_3 after the 967 cm^{-1} irradiation using a lens. We also observed a plume in this case. In addition to the plume formation, we noted a color change of the sample to black. As shown in Figures 6d-A, 6d-B, and 6d-C, products such as C_2H_4 and CH_3CHO were present in the gas phase. When the sample was irradiated at a slightly off-focal position, the color changed faintly and the production of C_2H_4 was small as seen in Figure 6d-A. When the sample was located more exactly at the focal position, the sample color was darker and production of C_2H_4 and CH_3CHO increased in Figure 6d-B and Figure 6d-C in that order. We observed the strongest plume at position (d-C) (Figure 6d). The rough intensity dependence indicated that the initiation of the conversion reaction required a threshold power density of FEL. A noteworthy point is the origin of the color change. Two origins for the color change can be proposed. One is carbon deposition after the reaction. Tono et al. reported that anthracene deposited on a NaCl substrate was tanned after FEL irradiation.[21] They analyzed the sample and discovered graphite sheet formation. They observed a white plume only after the sample was tanned. The other is reduction of the MoO_3. Reduced Mo_2O_5 is violet or blue, whereas MoO_3 is white.[22]

The former possibility is less likely because we observed a color change of the sample when the sample was irradiated without C_2H_5OH at 967 cm^{-1}. In order to obtain further evidence, we measured XPS to determine the surface chemical composition.

XPS. Figure 7 shows a wide scan of XPS spectra of MoO_3 before (a) and after (b) irradiation at 967 cm^{-1}. Fundamentally, no great difference was apparent in the wide-scan spectra. We observed the C1s peak in every sample with almost equal intensity. Thus, we were able to reject the possibility of graphite formation because no increase in carbon content was observed after irradiation. The Mo peak was broadened to the lower binding energy in the sample excited by 967 cm^{-1}, as shown in Figure 8b, indicating reduction of the Mo species after the irradiation at 967 cm^{-1}. The peak deconvolution analysis of $Mo3d_{5/2}$ as shown in Figure 8c indicated that two peaks appeared at 233 and 231.4 eV, which correspond to those of Mo^{6+} and Mo^{5+}.[23,24] The peak area ratios were 2:1. Thus, Mo^{5+} was the origin for the post-irradiation dark coloration.

Small shoulders were visible in the O1s spectrum after the reaction as shown in Figure 9. Peak deconvolution analysis indicated two peaks at 530.2 and 528.6 eV. The peak area ratio of the 528.6 eV peak to the 530.2 eV peak was about 1:4. The 530.2 eV peak can be assigned to lattice oxygen. However, it is difficult to assign the 528.6 eV peak. There are two possibilities to explain the peak. One is the oxygen bound to Mo^{5+}. However, the O1s peak is unchanged or shifted slightly to a higher binding energy when its central atom (Mo^{5+}) is reduced.[25] The other is surface OH groups which are found in XPS of oxide surfaces. But the O1s of the OH group appears at 2 eV higher than the lattice oxygen peak.[26] Thus, the 528.6 eV peak is not the case. Simply judging from the binding energy of O1s of 528.6 eV, the oxygen species should be more negatively charged: probably ionic oxygen. We are unable to assign the lower binding energy O1s peak and in situ experiments are necessary to determine the origin of negatively charged oxygen.

Discussion

Normally in thermal reaction on MoO_3, ethanol is converted mainly to acetaldehyde with a very small amount of $(C_2H_5)_2O$.[5] In fact, we can find only the production of CH_3CHO in the thermally excited case. On the other hand, IR-FEL irradiation gives C_2H_4 as its main product. This is one remarkable feature of IR-FEL-induced reaction. The reaction proceeds in a different manner from that of the conventional thermal reaction.

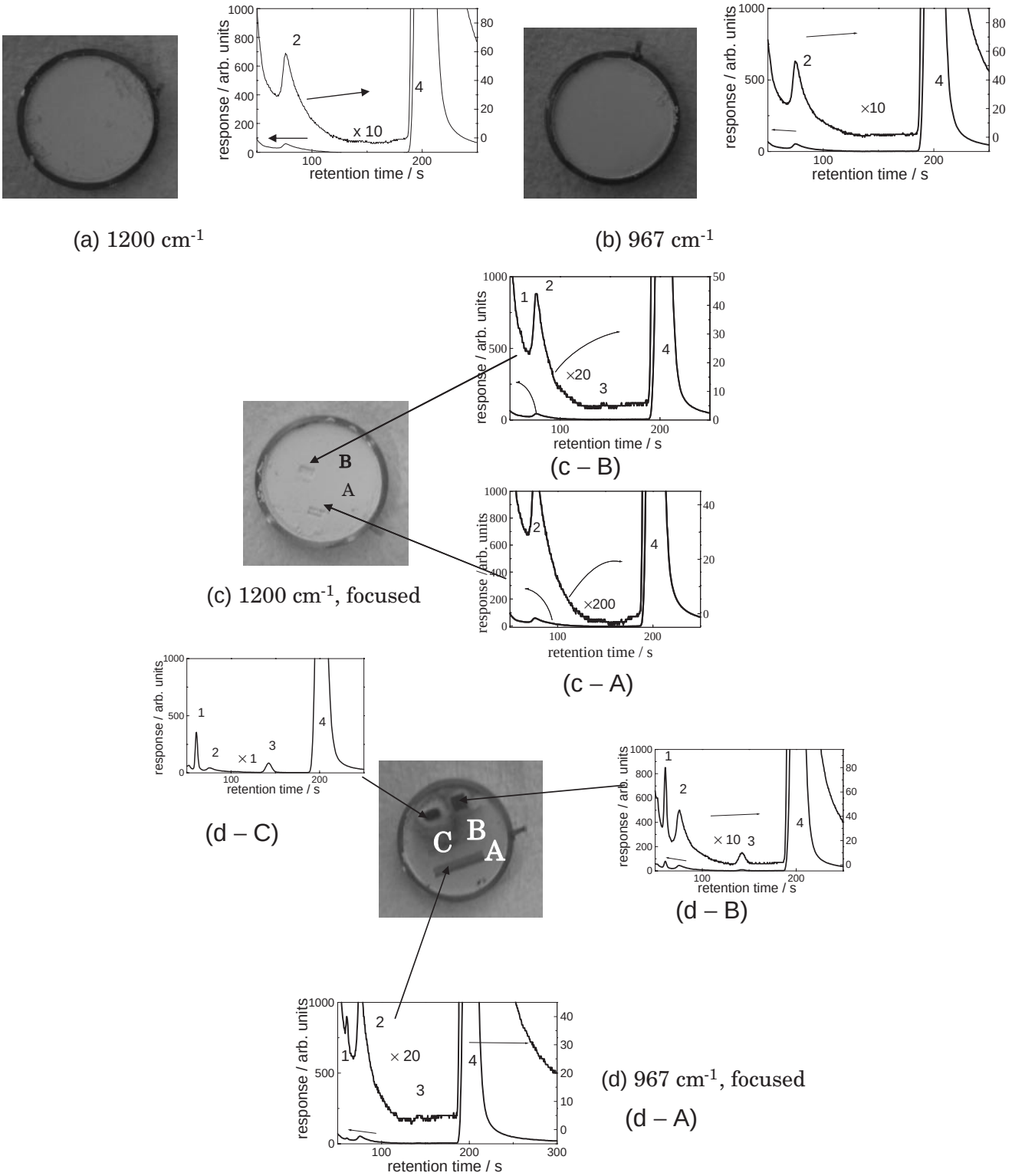

Figure 6. Photographs of the sample after the FEL irradiation and gas chromatography outputs. (a) and (b) were irradiated with 1200 and 967 cm^{-1} focused gently with a mirror, respectively. (c) and (d) were irradiated with 1200 and 967 cm^{-1} light focused strictly with a lens, respectively. (c-A), (c-B), (d-A), (d-B), and (d-C) indicate the positions with different focusing conditions. (c-B) and (d-C) were the cases in which the sample was placed at most strictly focused position while (c-A) and (d-A) were the ones with the mildest focusing conditions.

The second important feature of the present investigation is wavelength specificity. C_2H_4 was produced when the sample was irradiated with 967 cm^{-1} IR light. We found little product when we irradiated the sample at 1200 cm^{-1}, although the power was stronger than that at 967 cm^{-1}. We observed ethylene formation even at 814 cm^{-1}, whose IR power was half of

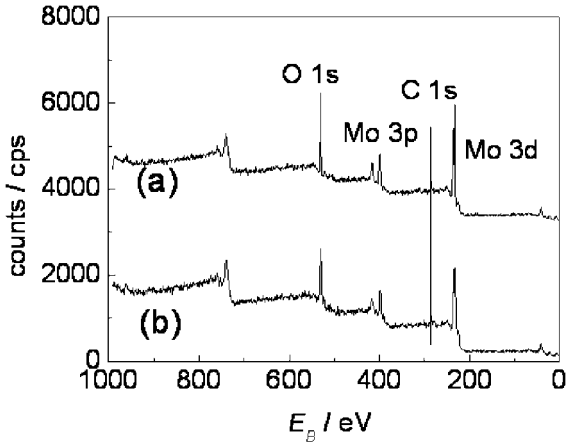

Figure 7. Wide scan XPS spectra of MoO_3 before (a) and after (b) infrared irradiation.

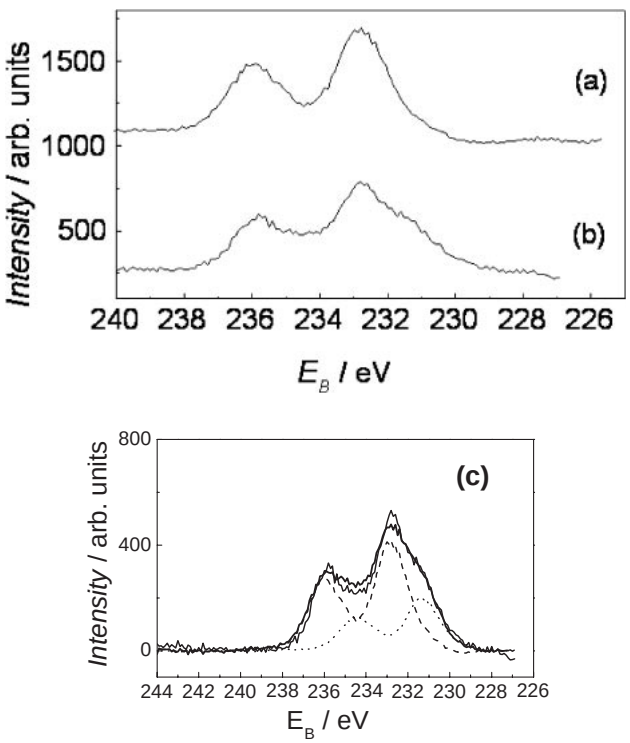

Figure 8. Mo3d XPS spectra of MoO_3 (a) before irradiation, (b) after irradiation at 967 cm^{-1} infrared FEL. (c) Peak deconvolution of Mo3d peaks into two Mo components. Broken and dotted lines: component XPS spectra, thin and thick lines: synthesized and observed data, respectively.

that at 1200 cm^{-1}. Both 967 and 814 cm^{-1} correspond respectively to $Mo(=O)_2$ asymmetric and symmetric vibration modes assuming C_{2v} local symmetry. Thus, the IR-FEL induces a reaction at the resonant wavelength of $Mo(=O)_2$.

The third is that the reaction has a threshold laser intensity. If the infrared beam was gently focused onto the sample, we observed neither a plume nor any reaction product. The plume consists of plasma that emits white light through several mechanisms.[21,27–33] Plasma is first created through ionization that occurs because of the strong electric field owing to several ion-

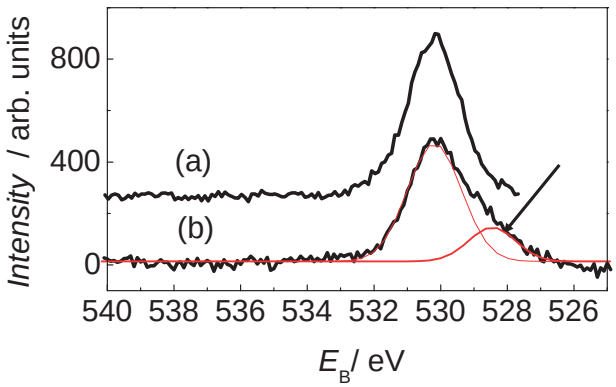

Figure 9. O1s XPS spectra of MoO_3 (a) before the irradiation, (b) after irradiation at 967 cm^{-1} infrared FEL. 528.6 eV feature is indicated by an arrow.

ization mechanisms such as (1) multiphoton ionization (MPI); (2) tunnel ionization (field ionization) (TI); and (3) thermoionization process. For whatever reason, an ionization occurs and a plume was produced on the MoO_3 as a result of the intense IR irradiation. However, the plume in itself yields little products as clarified in the case of 1200 cm^{-1} irradiation. That might be due to the low density of active species in the plasma and the amount of products was less than the detection limit.

The color change seems to be an important phenomenon related to the reaction. When the sample is irradiated with the 967 cm^{-1} beam, both color change and the reaction occur. The sample color change occurs only as a result of irradiation. Subsequent analysis by XPS reveals that the dark color originates not from carbon contamination but from Mo reduction. The MoO_3 is reduced by infrared irradiation. We observed a plume immediately after every infrared laser shot at 1200 cm^{-1}, indicating that the power was sufficient to create plasma while the color remained white. Therefore, the color change and plume formation are independent events of the irradiation process. Intense light not only induces ionization but also bond dissociation between Mo and O after multiphoton absorption and ladder climbing of the vibrational states.

$$2Mo^{6+}{=}O + nh\nu \rightarrow (Mo^{5+})_2O + O \quad (1)$$

As a result, reduced and coordinatively unsaturated Mo species are formed, which may reveal high activity. The C_2H_5OH dehydrogenation reaction occurs on the partially reduced Mo^{5+} species, which has been created by the IR-FEL. The IR-FEL tuned at the Mo=O wavelength is important for dissociation of the Mo=O bond and reduction of Mo^{6+}.

Our original aim was to excite the Mo–O bond and provoke selective reaction. For this purpose we used a pulse infrared light, IR-FEL, in order to distinguish laser-driven reactions from thermal ones. We found the resonant IR wavelengths on specific vibrational modes of MoO_3 could initiate a reaction. However, simple single photon absorption could not induce the reaction. Focusing of intense IR light was essential for the reaction, suggesting that multiphoton absorption is involved. Before the experiment we were afraid that intense IR light might induce optical breakdown and plasma which would make reaction control difficult. However, the current reaction was not the case; plasma might not be a key phenomenon

for the oxidation reaction of C_2H_5OH on MoO_3. Instead the selective bond cleavage by the multiphoton absorption is important for the further reaction. This finding can open a possibility to create a new active site by IR-FEL irradiation. For example, Ni_2P catalyst is active for hydrodesulfurization reaction.[34] EXAFS investigation revealed that the active phase is NiP_xS_y which is created during the reaction.[35–37] There are several Ni–P bond in this catalyst.[38,39] If a Ni–P bond is selectively activated by IR-FEL and is substituted with a Ni–S bond, one may know which Ni–P and Ni–S bonds are important and prepare more active catalysts effectively.

Conclusion

Our study has first demonstrated that pulse IR-FEL excites a Mo–O bond and activates a reaction path that is different from that excited thermally. The multiphoton excitation of the Mo–O bond at a resonance frequency dissociated the Mo–O bonds and created an active Mo^{5+} state where dehydration reaction occurs. In addition, the plasma seems to be ineffective for C_2H_5OH dehydration and dehydrogenation reactions.

One author (MGM) expresses his appreciation to the Japanese Society for the Promotion of Science (JSPS) for financial support from the postdoctoral Fellowship for Foreign Researchers Program. The research was partially supported by a Grant-in-Aid for Scientific Research Category S (No. 16106010) and for Creative Scientific Research of Japan Society of Promotion of Science (No. 11NP0101) of JSPS. The authors thank the technical staff of the Catalysis Research Center at Hokkaido University for their contribution to the construction of the measurement equipment. We thank all staff of FEL-TUS, especially Dr. T. Imai and Prof. A. Iwata for their technical assistance and Dr. H. Kondo, Dr. K. Tono, and Prof. T. Ohta (the University of Tokyo) for their discussion.

References

1 *Handbook of Heterogeneous Catalysis*, ed. by J. Haber, G. Ertl, H. Knozinger, VCH, Weinheim, **1997**, Vol. 5, p. 2253.
2 P. Mars, D. W. van Krevelen, *Chem. Eng. Sci., Spec. Suppl.* **1954**, *3*, 41.
3 J. C. Volta, W. Desquesnes, B. Moraweck, J. M. Tatibouet, Proceedings of the 7th International Congress on Catalysis, Tokyo, **1981**, p. 1398.
4 J. C. Volta, J. M. Tatibouet, *J. Catal.* **1985**, *93*, 467.
5 J. M. Tatibouet, J. E. Germain, J. C. Volta, *J. Catal.* **1983**, *82*, 240.
6 M. R. Smith, U. S. Ozkan, *J. Catal.* **1993**, *141*, 124.
7 L. Kihlborg, *Ark. Kemi.* **1963**, *21*, 357.
8 W. J. Chun, K. Ijima, Y. Ohminami, S. Suzuki, K. Asakura, *J. Synchrotron Radiat.* **2004**, *11*, 291.
9 J. Ziółkowski, *J. Catal.* **1983**, *81*, 311.
10 J. Ziółkowski, *J. Catal.* **1986**, *100*, 45.
11 M. A. Py, P. E. Schmid, J. T. Vallin, *Il Nuovo Cimento* **1977**, *38*, 271.
12 M. A. Py, K. Maschke, *Physica B+C* **1981**, *105*, 370.
13 H. Motz, W. Thon, R. N. Whitehurst, *J. Appl. Phys.* **1953**, *24*, 826.
14 J. M. M. Madey, *J. Appl. Phys.* **1971**, *42*, 1906.
15 H. Kuroda, K. Nakai, M. Kawai, K. Nomaru, in *Free Electron Lasers 2002*, ed. by K.-J. Kim, S. V. Milton, E. Gluski, Elsevier Science, B.V., Amsterdam, **2003**, Vol. II, p. 21.
16 S. Sato, H. Niimi, S. Suzuki, W.-J. Chun, K. Irokawa, H. Kuroda, K. Asakura, *Chem. Lett.* **2004**, *33*, 558.
17 Z. Liu, L. C. Feldman, N. H. Tolk, Z. Zhang, P. I. Cohen, *Science* **2006**, *312*, 1024.
18 M. Yokoyama, F. Oda, K. Nomaru, H. Koike, M. Sobajima, H. Miura, M. Kawai, H. Kuroda, *Nucl. Instrum. Methods Phys. Res., Sect. A* **2002**, *483*, 291.
19 F. Oda, M. Yokoyama, M. Kawai, H. Miura, H. Koike, M. Sobajima, K. Nomaru, H. Kuroda, *Jpn. J. Appl. Phys.* **2002**, *41*, 414.
20 W. J. Chun, K. Asakura, H. Ishii, T. Liu, Y. Iwasawa, *Top. Catal.* **2002**, *20*, 89.
21 K. Tono, H. Kondoh, Y. Hamada, T. Suzuki, K. Bito, T. Ohta, S. Sato, H. Hamaguchi, A. Iwata, H. Kuroda, *Jpn. J. Appl. Phys.* **2005**, *44*, 7561.
22 R. C. Weast, J. A. Melvin, *Handbook of Chemistry and Physics*, 63rd ed., **1982–1983**.
23 W. E. Swartz, Jr., D. M. Hercules, *Anal. Chem.* **1971**, *43*, 1774.
24 K. Asakura, K. Nakatani, T. Kubota, Y. Iwasawa, *J. Catal.* **2000**, *194*, 309.
25 H. S. Potdar, A. B. Mandale, S. D. Sathaye, A. P. B. Sinha, *J. Mater. Sci.* **1987**, *22*, 2023.
26 D. Y. Zemlyanov, E. Savinova, A. Scheybal, K. Doblhofer, R. Schloegl, *Surf. Sci.* **1998**, *418*, 441; L.-Q. Wang, K. F. Ferris, A. N. Shultz, D. R. Baer, M. H. Engelhard, *Surf. Sci.* **1997**, *380*, 352.
27 E. A. Rohlfing, *J. Chem. Phys.* **1988**, *89*, 6103.
28 T. Sakka, S. Iwanaga, Y. H. Ogata, A. Matsunawa, T. Takemoto, *J. Chem. Phys.* **2000**, *112*, 8645.
29 Y. Tasaka, M. Tanaka, S. Usami, *Jpn. J. Appl. Phys.* **1995**, *34*, 1673.
30 F. Varga, L. Nemes, *J. Mol. Struct.* **1999**, *480–481*, 273.
31 D. M. Simanovskii, H. A. Schwettman, H. Lee, A. J. Welch, *Phys. Rev. Lett.* **2003**, *91*, 107601.
32 G. Von Helden, I. Holleman, A. J. A. Van Roij, G. M. H. Knippels, A. F. G. van der Meer, G. Meijer, *Phys. Rev. Lett.* **1998**, *81*, 1825.
33 T. Leisner, K. Athanassenas, D. Kreisle, E. Recknagel, *J. Chem. Phys.* **1993**, *99*, 9670.
34 S. T. Oyama, *J. Catal.* **2003**, *216*, 343.
35 S. T. Oyama, X. Wang, Y.-K. Lee, W.-J. Chun, *J. Catal.* **2004**, *221*, 263.
36 T. Kawai, K. K. Bando, Y. K. Lee, S. T. Oyama, W. J. Chun, K. Asakura, *J. Catal.* **2006**, *241*, 20.
37 A. E. Nelson, M. Sun, A. S. M. Junaid, *J. Catal.* **2006**, *241*, 180.
38 J. A. Rodriguez, J. Y. Kim, J. C. Hanson, S. J. Sawhill, M. E. Bussell, *J. Phys. Chem. B* **2003**, *107*, 6276.
39 M. G. Moula, S. Suzuki, W. J. Chun, S. Otani, S. T. Oyama, K. Asakura, *Chem. Lett.* **2006**, *35*, 90.